



Brazilian Journal of Physics

ISSN: 0103-9733

luizno.bjp@gmail.com

Sociedade Brasileira de Física
Brasil

Garitezi, T. M.; Adriano, C.; Rosa, P. F. S.; Bittar, E. M.; Bufaical, L.; de Almeida, R. L.; Granado, E.; Grant, T.; Fisk, Z.; Avila, M. A.; Ribeiro, R. A.; Kuhns, P. L.; Reyes, A. P.; Urbano, R. R.; Pagliuso, P. G.

Synthesis and Characterization of BaFe₂As₂ Single Crystals Grown by In-flux Technique

Brazilian Journal of Physics, vol. 43, núm. 4, agosto, 2013, pp. 223-229

Sociedade Brasileira de Física

São Paulo, Brasil

Available in: <http://www.redalyc.org/articulo.oa?id=46427890003>

- How to cite
- Complete issue
- More information about this article
- Journal's homepage in redalyc.org

redalyc.org

Scientific Information System

Network of Scientific Journals from Latin America, the Caribbean, Spain and Portugal

Non-profit academic project, developed under the open access initiative

Synthesis and Characterization of BaFe_2As_2 Single Crystals Grown by In-flux Technique

T. M. Garitezi · C. Adriano · P. F. S. Rosa · E. M. Bittar ·
L. Bufaical · R. L. de Almeida · E. Granado · T. Grant ·
Z. Fisk · M. A. Avila · R. A. Ribeiro · P. L. Kuhns ·
A. P. Reyes · R. R. Urbano · P. G. Pagliuso

Received: 13 May 2013 / Published online: 9 July 2013
© Sociedade Brasileira de Física 2013

Abstract We report a detailed characterization of BaFe_2As_2 single crystals grown by a metallic In-flux technique, an alternative to well-established growth routes using FeAs self- or Sn-flux. Electrical resistivity, magnetic susceptibility, nuclear magnetic resonance, and energy dispersive spec-

troscopy measurements showed no evidence of flux incorporation. More importantly, our results demonstrate that BaFe_2As_2 single crystals grown by In-flux have extremely high quality. To explore the efficiency of the In-flux growth method, we have also prepared nearly optimally doped superconducting samples of $\text{Ba}(\text{Fe}_{1-x}\text{M}_x)_2\text{As}_2$ ($\text{M} = \text{Co}, \text{Cu}, \text{Ni}, \text{and Ru}$). Among other interesting features, this alternative chemical substitution method has led to enhancement of the maximum T_c for most dopings.

T. M. Garitezi · C. Adriano · P. F. S. Rosa · E. M. Bittar ·
L. Bufaical · R. L. de Almeida · E. Granado · R. R. Urbano ·
P. G. Pagliuso (✉)
Instituto de Física “Gleb Wataghin”, UNICAMP, 13083-859
Campinas, São Paulo, Brazil
e-mail: pagliuso@ifi.unicamp.br

T. M. Garitezi
e-mail: thalesmg@ifi.unicamp.br

E. M. Bittar
Centro Brasileiro de Pesquisas Físicas,
22290-180 Rio de Janeiro, Rio de Janeiro, Brazil

L. Bufaical
Instituto de Física, Universidade Federal de Goiás,
C. P. 131, 74001-970 Goiânia, Goiás, Brazil

E. Granado
Laboratório Nacional de Luz Síncrotron,
C. P. 6192, 13083-970 Campinas, São Paulo, Brazil

T. Grant · Z. Fisk · P. G. Pagliuso
University of California,
Irvine, CA 92697-4573, USA

M. A. Avila · R. A. Ribeiro
Centro de Ciências Naturais e Humanas,
Universidade Federal do ABC,
09210-580 Santo André, São Paulo, Brazil

P. L. Kuhns · A. P. Reyes · R. R. Urbano
National High Magnetic Field Laboratory,
Florida State University,
Tallahassee, FL 32306-4005, USA

Keywords Superconductivity · Pinictides ·
Antiferromagnets · Conduction · Crystal growth

1 Introduction

Iron-based superconductors were discovered a few years ago and have been attracting great interest in the scientific community. Particularly extensive work has been dedicated to understanding the microscopic interplay between superconductivity and magnetism, which is believed to mediate the emergence of superconductivity in these materials [1–3]. One of the most studied compounds in this novel family of high- T_c superconductors is the parent BaFe_2As_2 (namely Ba122), a material with rich physical properties. For instance, chemical substitution of Ba, Fe, and/or As by a number of other elements as well as the application of hydrostatic pressure can monotonically suppress the spin-density wave (SDW) magnetic order and induce superconductivity (SC). In general, the SC phase emerges near the suppression of SDW order, and in certain cases, microscopic coexistence becomes possible in a range of doping and pressure [1–3]. The superconducting critical field (H_{c2}) for these materials is surprisingly high, usually of the order of 100 T. All these features make this family of materials

extremely interesting for both academic and technological applications.

Proper study of microscopic properties, which may be related to the aforementioned phenomena, calls for single crystals with as good quality as possible. Extrinsic effects such as impurities, defects, etc. can modify the intrinsic properties of these compounds and have often lead to erroneous conclusions. In particular, in the case of compounds with distinct ground states (e.g., SDW and SC), extrinsic effects can modify the phase diagram by subtly tuning their response to applied pressure and/or doping.

The most popular methods to grow Ba122 single crystals are the Sn-flux and self-flux (excess of FeAs) techniques. These procedures introduce an excess of flux material into the crucible, which facilitates the nucleation of single crystals [4]. On the one hand, Sn-flux can produce very large single crystals, which are appropriate for neutron and thermodynamic experiments. On the other hand the self-flux method introduces no other elements in the melt and so, in principle, should yield the purest single crystals. Notwithstanding these advantages, certain drawbacks associated with the two techniques deserve mention: Sn-flux samples have shown evidence of flux incorporation [5], which has altered their physical properties and introduced considerable inhomogeneity; self-flux samples can present stoichiometric variations from 1-2-2 due to the excess of FeAs in the melt. And worse, the excess As in the self-flux growth exposes growers to an additional chemical hazard, given the much larger amounts of As handled in the process.

Here, we present a detailed investigation of metallic In-flux-grown (IFG) BaFe₂As₂ single crystals. Our single crystals show no trace of In-flux incorporation. The results of transport, magnetic, thermodynamical, nuclear magnetic resonance (NMR), and structural measurements indicate that the samples grown by In-flux have equal or, in most cases, higher crystallographic quality than those grown by self-flux (SFG) and Sn-flux (TFG). The larger size and higher quality of the crystals harvested from the alternative method constitute great improvement over the other procedures and make the samples more suitable for a myriad of experimental techniques.

2 Experimental Details

Single crystals of Ba(Fe_{1-x}M_x)₂As₂ ($M = \text{Co, Cu, Ni, and Ru}$) were grown from In-rich flux. Elemental Ba, (Fe, M), and As were added to In in the ratio of Ba/(Fe, M)/As/In = 1:2:2:25. The materials were placed in alumina crucibles and sealed in quartz tubes in vacuum. To optimize incorporation, we used a special heat treatment for each dopant. The materials were heated up to the top temperature T_{top} in conventional furnaces for a time t_{top} , then slowly cooled

at a rate r down to the removal temperature T_{rem} , when the tubes were centrifuged to eliminate excess In. Table 1 shows the parameters for the pure compound and for different dopants (Co, Cu, Ni, and Ru). The resultant crystals were shiny platelets with typical dimensions ranging from $0.5 \times 0.5 \times 0.05$ to $3.0 \times 3.0 \times 0.05$ mm³ for all samples. A photograph of one of the largest crystals obtained by this method is shown in Fig. 1. The crystals were characterized by x-ray powder diffraction and submitted to elemental analysis using a commercial energy dispersive spectroscopy (EDS) microprobe. Electrical resistivity was measured with a Quantum Design PPMS. A standard four-probe technique was used in resistivity measurements. Magnetic susceptibilities were measured with a Quantum Design MPMS. NMR experiments were carried out at the National High Magnetic Field Laboratory in Tallahassee, FL, USA, using a NMR probe equipped with a goniometer for fine in situ alignment of the crystallographic axes with the external applied magnetic field. The field-swept ⁷⁵As NMR spectra ($I = 3/2$; $\gamma/2\pi = 7.2919$ MHz/T) were obtained by stepwise summing the Fourier transform of the spin-echo signals. High-resolution synchrotron x-ray diffraction measurements were made at the XPD beamline of the Brazilian Synchrotron Light Laboratory (LNLS) [6], with $\lambda = 1.23984$ Å. The sample was placed in the cold finger of a closed-cycle He cryostat, which was mounted in the Eulerian circle of a commercial $4 + 2$ circle diffractometer. A Ge(111) analyzer crystal was used in the 2θ arm to improve the angular resolution of the diffracted beam.

3 Results and Discussion

We first describe the electrical resistivity data obtained from our BaFe₂As₂ single crystals, grown by In-flux. We compare the data with previous reports on the resistivity of similar samples grown by other methods.

Figure 2 shows the temperature dependence of the in-plane resistivity ρ_{ab} for pure BaFe₂As₂ crystals. The crystals grown by In-flux present a sharp feature at $T_0 \simeq 139$ K, signaled by the peak in the derivative $d\rho_{ab}/dT$. In opposition to the thermal dependence observed in TFG samples,

Table 1 Heat treatment parameters for optimized growth of pure and doped BaFe₂As₂, with different dopants (see text)

Doping atom	T_{top} (°C)	t_{top} (h)	r (°C/h)	T_{rem} (°C)
Pure	1,100	18	10	400
Co	1,100	18	10	400
Cu	1,100	21	3	550
Ni	1,100	18.5	10	400
Ru	1,150	12	2	550

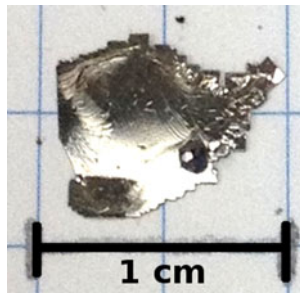


Fig. 1 (Colored online) Photograph of one of the largest pure single crystals obtained by In-flux growth technique

the resistivity drops monotonically as the temperature is decreased below T_0 . Our In-flux samples displayed residual resistivity ratios ranging from 6 to 8. This agrees with the ratios found in samples grown by self-flux [7] as well as in a polycrystalline sample [8]. The residual resistivity was found to be typically $\rho_0 \approx 0.1$ m Ω -cm for the IFG samples, comparable to the residual resistivities reported for SFG samples [9–11].

Figure 2 clearly shows that the TFG crystal deviates from this behavior. For decreasing temperatures, the resistivity crosses 139 K with no special feature, and there is a broad rise, rather than decay, in the resistivity around 85 K. This is indicative of Sn incorporation, as reported by Su et al. [5]. The temperature dependence of the resistivity in the IFG samples is analogous to the thermal dependence in the SFG samples, an indication that In has not been incorporated. EDS experiments (not shown) have also detected no In in our IFG single crystals.

Nuclear magnetic resonance (NMR) and nuclear quadrupolar resonance are powerful techniques providing

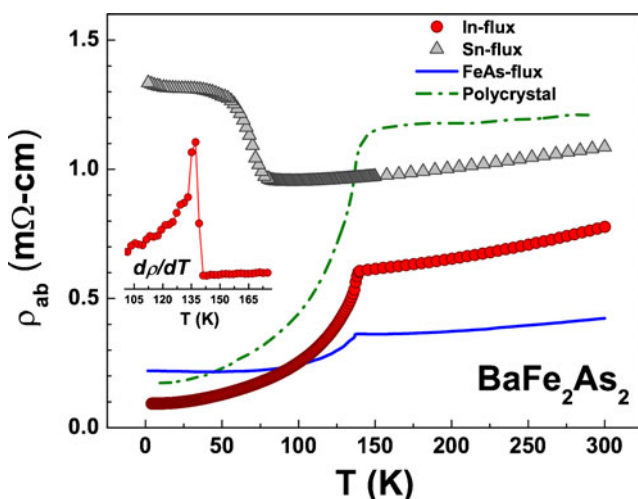


Fig. 2 (Colored online) In-plane resistivity as a function of temperature for BaFe_2As_2 single crystals grown by In- and Sn-flux. For comparison, we also show the resistivity of the self-flux [7] and polycrystalline [8] samples

information on the local structural and electronic environment in a lattice [12–15]. With this in mind, we have carried out ^{75}As NMR experiments to check the doping effects and sample quality. NMR lineshapes being usually affected by disorder and inhomogeneity, the linewidth is a reliable local probe of both effects. More specifically, the structure of the spectra describes the local environment of the ^{75}As sites.

Figure 3 shows the ^{75}As NMR signal for single crystals, grown by In- and Sn-flux, at 150 K with $H \perp c$. The central line corresponds to the $(1/2 \leftrightarrow -1/2)$ transition, and the satellites are $(\pm 3/2 \leftrightarrow \pm 1/2)$ transitions split by quadrupolar effects [15, 16]. The IFG sample shows a very narrow (5 kHz) central linewidth with no other peaks than the two satellites, whereas the TFG sample displays a broad central line with multiple peaks. Broad lines and multiple peaks are signatures of a local internal magnetic field distribution on top of possible As-site distribution and hence indicate low crystallographic quality. Previously reported NMR linewidths for SFG and TFG crystals are similar to or even larger than ours [16–18]. Furthermore, the BaFe_2As_2 samples from Refs. [17, 18] display several central transition peaks. These results offer microscopic proof that our IFG samples are as homogeneous as or more homogeneous than the SFG and TFG samples and signal improvement in the preparation of Fe-arsenide compounds.

High-resolution synchrotron X-ray powder diffraction measurements on IFG BaFe_2As_2 were made at the Brazilian LNLS. Figure 4a shows $\theta - 2\theta$ scans in the vicinity of the

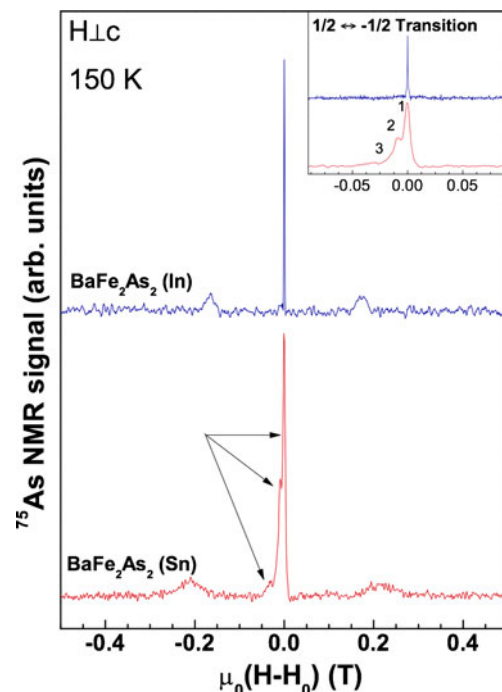


Fig. 3 (Colored online) ^{75}As NMR signal for BaFe_2As_2 single crystals grown by In- and Sn-flux in the paramagnetic (tetragonal) phase

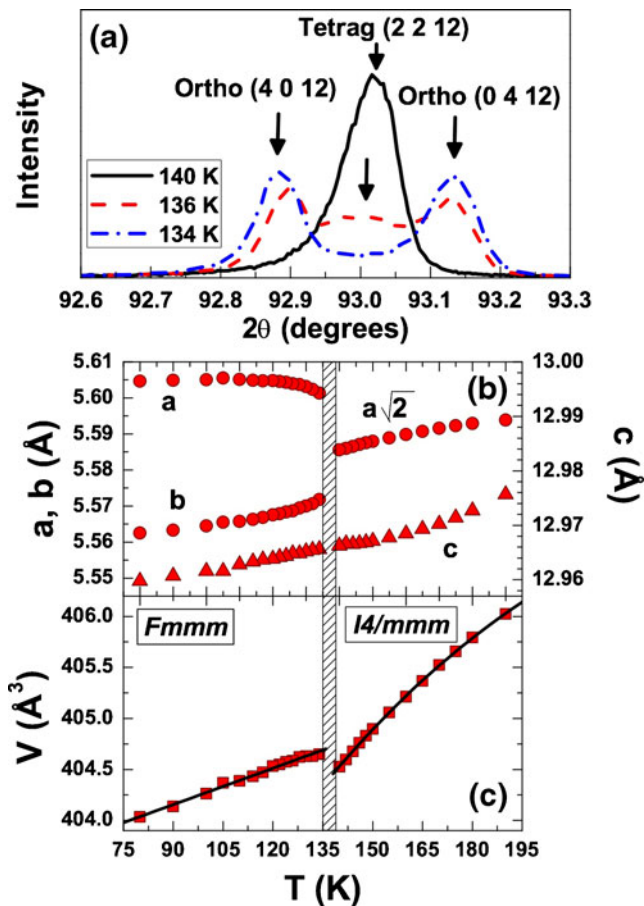


Fig. 4 (Colored online) High-resolution synchrotron X-ray diffraction of a IFG BaFe_2As_2 single crystal. **a** Radial ($\theta - 2\theta$) scans around the (2 2 12) tetragonal reflection. **b** Temperature dependence of the a , b , and c lattice parameters. **c** Temperature dependence of the unit cell volume

(2 2 12) reflection of the tetragonal structure (space group $I4/mmm$). A splitting of this reflection upon cooling below ~ 139 K is observed, consistent with the emergence of the orthorhombic phase (space group $Fmmm$). Tetragonal and orthorhombic reflections coexist over a small temperature range of ~ 4 K. The coexistence has also been observed in NMR experiments [15, Garitezi et al. unpublished].

Figure 4b shows the temperature evolution of the a , b , and c lattice parameters, obtained from the diffraction signal in Fig. 4a and from the (006) reflection (not shown), indicating a sharp structural transition. A small cell volume discontinuity can be discerned at the transition, as Fig. 4c shows. The jump suggests that the transition is of first order, as pointed out by previous authors [2].

In order to evaluate the efficiency of the In-flux method here proposed to grow Ba122 compounds, we have also synthesized doped $\text{Ba}(\text{Fe}_{1-x}\text{M}_x)_2\text{As}_2$ ($M = \text{Co}, \text{Cu}, \text{Ni}, \text{and Ru}$) single crystals. Although we have produced a wide range of chemical substitutions for Co doping, we will here

focus on the optimally doped samples, i. e., the superconducting samples with maximum T_c and with completely suppressed magnetic SDW state, for $M = \text{Co}, \text{Ni}$ and Ru .

Figure 5 displays the temperature dependence of the in-plane resistivity for different M -doped Ba122 compounds. Figure 5a shows that the alternative In-flux route also yields bulk superconducting samples for Co, Cu, Ni, and Ru doping, in agreement with previous reports for samples grown by the self- and Sn-flux techniques [19–27]. A noteworthy sign of improvement over the SFG technique is the overall higher maximum T_c . Except for Ru, the IFG crystals show maximum T_c 's that are higher than those for the corresponding SFG samples. Moreover, the residual resistivity ρ_0 at T_c , ranges from 0.2 to 1.0 mΩ-cm, equal to or smaller than

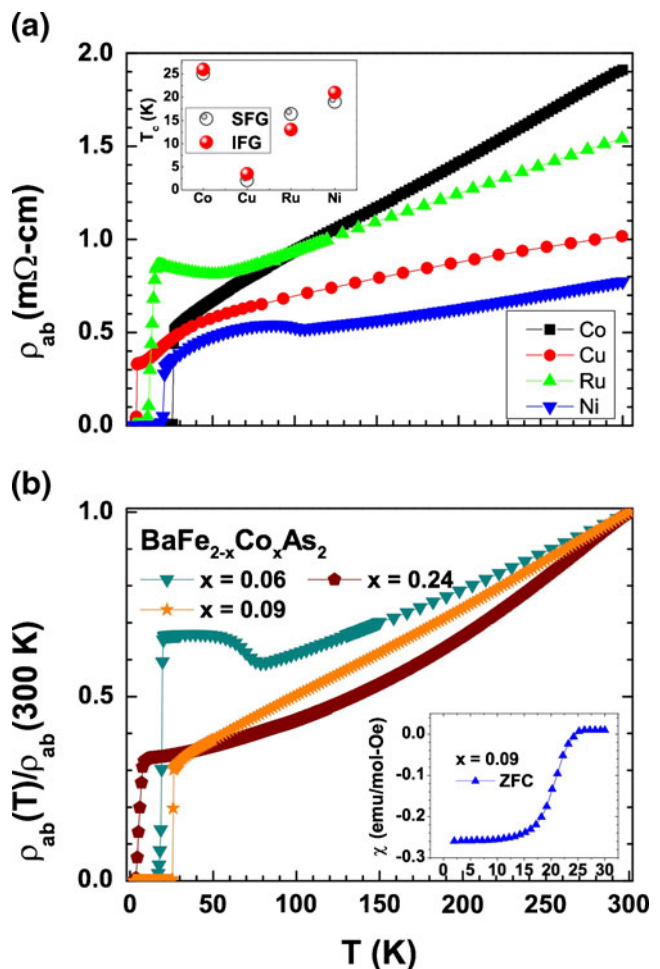


Fig. 5 (Colored online) **a** In-plane electrical resistivity as a function of temperature for $\text{Ba}(\text{Fe}_{1-x}\text{M}_x)_2\text{As}_2$ single crystals grown by In-flux ($M = \text{Co}, \text{Cu}, \text{Ni}, \text{and Ru}$). Each curve was obtained from the sample with the highest T_c in its batch. The inset shows the maximum T_c 's for self- and In-flux-grown crystals with various dopants [24–27]. **b** In-plane electrical resistivity as a function of temperature for $\text{Ba}(\text{Fe}_{1-x}\text{Co}_x)_2\text{As}_2$ IFG single crystals ($x = 0.03, 0.045, \text{and } 0.12$). The inset shows the zero-field-cooled (ZFC) magnetic susceptibility for the optimally doped sample ($x = 0.045$)

the residual resistivities for previous reports on other samples [19–23]. We note, however, that our growth procedure for Ru-substituted compounds is not yet fully optimized, as indicated by the reduced crystal size.

Ru doping aside, it is plausible to assume that the IFG samples have higher critical temperatures because they contain a reduced number of defects that are nonmagnetic pair-breaking centers. We therefore strongly believe that the physical properties of IFG samples are less prone to be significantly affected by the interference of defects and inhomogeneity. The IFG samples are hence more suitable for microscopic investigations.

Let us now turn our attention to Co-doped BaFe_2As_2 , which has generated the largest doped IFG single crystals so far. On the basis of transport data, such as the results in Fig. 5b, we have constructed the phase diagram in Fig. 6.

Although the T - x phase diagram in Fig. 6, for our Co-doped Ba122, is qualitatively similar to the diagram in Ref. [24] and, to the best, the maximum T_c (26 K) exceeds all previously reported critical temperatures.

The critical current J_c also measures the quality of a superconducting material. A well-established way to estimate J_c employs the Bean model of magnetization loops [28]. Accordingly, to estimate the critical current J_c , we have studied the magnetization of several Co-doped IFG samples in detail. The J_c 's extracted from the ΔM 's at zero field and $T = 2$ K lie within the range 6×10^3 – 3×10^6 A/cm² for magnetization loops with $H \perp c$. These critical currents are smaller than those obtained for Co-doped SFG samples over the entire doping range [29–34].

The critical current of a superconducting sample estimated by the Bean model is limited by the average pinning strength, which increases with defect concentration. Smaller

critical currents and the same range of residual resistivities are indicative of a sample with equal or lower defect concentration. We have also studied critical-current transport in our crystals and obtained values about 2 orders of magnitude smaller than the Bean model estimates. The details of this study, which are beyond the scope of this work, will be reported elsewhere (Garitezi et al. unpublished).

Finally, since Co-dilution studies are frequently used to investigate Fe-based superconductors, it is important to determine the distribution of the Co atoms within the unit cell. We rely on a statistical model for the distribution of nearest-neighbor Co atoms in $\text{Ba}(\text{Fe}_{1-x}\text{Co}_x)_2\text{As}_2$ to estimate the relative Co concentration.

⁷⁵As NMR experiments were performed on Co-doped IFG single crystals, as shown in Fig. 7 for $\text{BaFe}_{1.989}\text{Co}_{0.011}\text{As}_2$ and $\text{BaFe}_{1.90}\text{Co}_{0.10}\text{As}_2$. For the latter material, a secondary peak arises near the central transition. The spectral structure reflects the local environment of the ⁷⁵As sites and corresponds to the homogeneous substitution of Co for the Fe atoms. The relative intensities of the peaks correspond to a simple binomial distribution [35]. By fitting the intensity of the two central peaks and comparing the result to a binomial distribution of Co dopants [36], we estimate a concentration of $x = 0.08(1)$ for $\text{BaFe}_{2-x}\text{Co}_x\text{As}_2$. Since this statistical estimate agrees well with the nominal concentration of $x = 0.10$, we can assume that the

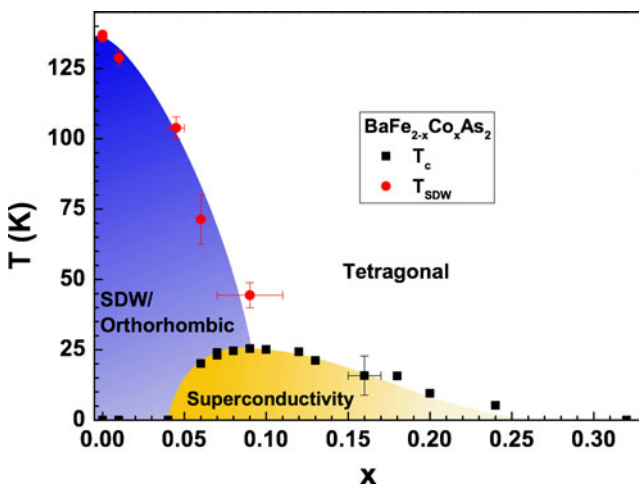


Fig. 6 (Colored online) T - x phase diagram for IFG $\text{BaFe}_{2-x}\text{Co}_x\text{As}_2$ single crystals. The error bars represent variations in the doping levels x and T_c amongst different batches with the same nominal Co content

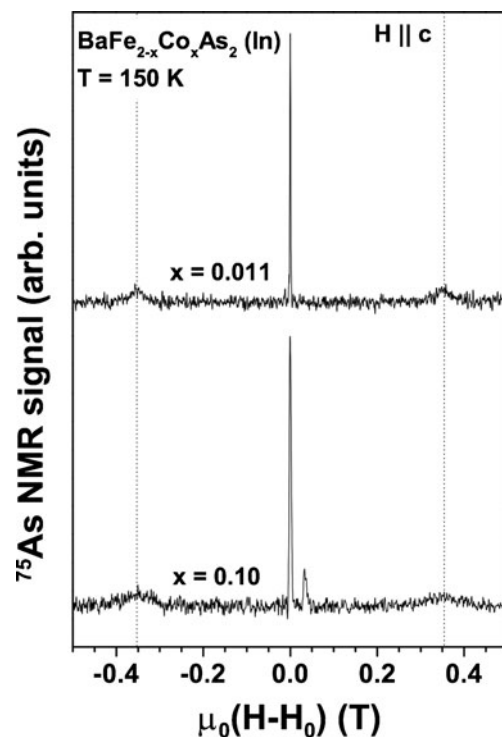


Fig. 7 ⁷⁵As NMR spectra for IFG, $\text{BaFe}_{1.989}\text{Co}_{0.011}\text{As}_2$, and $\text{BaFe}_{1.90}\text{Co}_{0.10}\text{As}_2$ for $H \perp c$ at 150 K (PM state) and $H = 13$ T

doping is homogeneously distributed throughout the lattice. This procedure yields a more reliable measure of the relative Co concentration than EDS, unsuitable because the Fe K_β overlaps with the Co K_α . The NMR linewidth for the Co-doped IFG crystals in the paramagnetic state at 150 K was found to be 6 kHz, narrower than the widths in SFG samples [37].

4 Conclusions

In summary, we have used an improved In-flux method to grow pure and doped BaFe₂As₂ single crystals. Diverse experimental techniques have ruled out In-flux incorporation into the crystals and revealed extremely high-quality samples. The residual resistivity ρ_0 of our IFG samples is comparable to the resistivities of SFG samples, which indicates at least similar sample quality. The superconducting critical currents J_c estimated from the magnetizations measured in our Co-doped crystals are reduced, which indicates lower concentration of pinning defects. In addition, the much narrower ⁷⁵As NMR linewidths of the IFG samples offer strong microscopic evidence of small defect and impurity concentrations. We have also shown that samples with different atom substitutions can be grown by the In-flux technique, leading to higher maximal critical temperatures T_c due to enhanced crystallographic homogeneity. Our main results suggest that the In-flux method can be extended to other chemical dopings and distinct families of iron-based superconductors. We expect other families, such as SrFe₂As₂ and CaFe₂As₂, to be within the reach of the method.

The Ba122 IFG crystals have already been the subject of several successful microscopic investigations [38–41], and the remarkable results are shedding new light on the relevant physical properties of those materials. In particular, quantum oscillations have been recently observed in transport and magnetization measurements of IFG BaFe₂As₂ and EuFe₂As₂ (Rosa et al. unpublished). We expect ongoing experiments to benefit from the higher quality of the improved IFG single crystals.

Acknowledgments This work was supported by the FAPESP (grant nos. 2006/60440-0, 2009/09247-3, 2010/11949-3, 2011/01564-0, 2011/23650-5, 2011/12292-0, 2012/04870-7, 2011/23795-3 and 2011/19924-2), CNPq, and NSF (in particular, DMR-0654118).

References

1. P. Paglione, R.L. Greene, *Nat. Phys.* **6**, 645 (2010)
2. G.R. Stewart, *Rev. Mod. Phys.* **83**, 1589 (2011)
3. P. Dai, J. Hu, E. Dagotto, *Nat. Phys.* **8**, 709 (2012)
4. Z. Fisk, J.P. Remeika, in *Handbook on the Physics and Chemistry of Rare Earth*, vol. 12, ed. K.A. Gschneidner Jr., L. Eyring, L.(Elsevier, Amsterdam, 1989), p. 53
5. Y. Su, P. Link, A. Schneidewind, Th. Wolf, P. Adelman, Y. Xiao, M. Meven, R. Mittal, M. Rotter, D. Johrendt, Th. Brueckel, M. Loewenhaupt, *Phys. Rev. B* **79**, 064504 (2009)
6. F.F. Ferreira, E. Granado, W. Carvalho Jr., S.W. Kycia, D. Bruno, R. Droppa Jr, *J. Synchrotron Rad.* **13**, 46 (2006)
7. A.S. Sefat, M.A. McGuire, R. Jin, B.C. Sales, D. Mandrus, F. Ronning, E.D. Bauer, Y. Mozharivskiy, *Phys. Rev. B* **79**, 094508 (2009)
8. M. Rotter, M. Tegel, D. Johrendt, I. Schellenberg, W. Hermes, R. Pöttgen, *Phys. Rev. B* **78**(R), 020503 (2008)
9. S. Ishida, T. Liang, M. Nakajima, K. Kihou, C.H. Lee, A. Iyo, H. Eisaki, T. Kakeshita, T. Kida, M. Hagiwara, Y. Tomioka, T. Ito, S. Uchida, *Phys. Rev. B* **84**, 184514 (2011)
10. M.A. Tanatar, N. Ni, A. Thaler, S.L. Bud'ko, P.C. Canfield, R. Prozorov, *Phys. Rev. B* **82**, 134528 (2010)
11. S.K. Kim, M.S. Torikachvili, E. Colombier, A. Thaler, S.L. Bud'ko, P.C. Canfield, *Phys. Rev. B* **84**, 134525 (2011)
12. E.D. Bauer, Y.-F. Yang, C. Capan, R.R. Urbano, C.F. Miclea, H. Sakai, F. Ronning, M.J. Graf, A.V. Balatsky, R. Movshovich, A.D. Bianchi, A.P. Reyes, P.L. Kuhns, J.D. Thompson, *Z. Fisk, PNAS* **108**, 6857 (2011)
13. R.R. Urbano, B.-L. Young, N.J. Curro, J.D. Thompson, L.D. Pham, Z. Fisk, *Phys. Rev. Lett.* **99**, 146402 (2007)
14. R.R. Urbano, E.L. Green, W.G. Moulton, A.P. Reyes, P.L. Kuhns, E.M. Bittar, C. Adriano, P.G. Pagliuso, *J. Phys. Conf. Ser.* **273**, 012107 (2011)
15. R.R. Urbano, E.L. Green, W.G. Moulton, A.P. Reyes, P.L. Kuhns, E.M. Bittar, C. Adriano, T.M. Garitezi, L. Bufaical, P.G. Pagliuso, *Phys. Rev. Lett.* **105**, 107001 (2010)
16. K. Kitagawa, N. Katayama, K. Ohgushi, M. Yoshida, M. Takigawa, *J. Phys. Soc. Jpn.* **77**, 114709 (2008)
17. A.P. Dioguardi, N. apRoberts-Warren, A.C. Shockley, S.L. Bud'ko, N. Ni, P.C. Canfield, N.J. Curro, *Phys. Rev. B* **82**(R), 140411 (2010)
18. S.-H. Baek, T. Klimczuk, F. Ronning, E.D. Bauer, J.D. Thompson, N.J. Curro, *Phys. Rev. B* **78**, 212509 (2008)
19. J.-P. Reid, M.A. Tanatar, X.G. Luo, H. Shakeripour, N. Doiron-Leyraud, N. Ni, S.L. Bud'ko, P.C. Canfield, R. Prozorov, L. Taillefer, *Phys. Rev. B* **82**, 064501 (2010)
20. N. Yasuyuki, T. Toshihiro, T. Yuji, T. Tsuyoshi, K. Hisashi, M. Takeshi, *Phys. Rev. B* **82**, 220504 (2010)
21. N. Ni, M.E. Tillman, J.-Q. Yan, A. Kracher, S.T. Hannahs, S.L. Bud'ko, P.C. Canfield, *Phys. Rev. B* **78**, 214515 (2008)
22. M.A. Tanatar, N. Ni, A. Thaler, S.L. Bud'ko, P.C. Canfield, R. Prozorov, *Phys. Rev. B* **82**, 134528 (2010)
23. E. Arushanov, G. Fuchs, S. Levchenko, S.L. Drechsler, B. Holzapfel, L. Schultz, *Supercond. Sci. Technol.* **24**, 105004 (2011)
24. H. Xiao, T. Hu, S.K. He, B. Shen, W.J. Zhang, B. Xu, K.F. He, J. Han, Y.P. Singh, H.H. Wen, X.G. Qiu, C. Panagopoulos, C.C. Almasan, *Phys. Rev. B* **86**, 064521 (2012)

25. A. Thaler, N. Ni, A. Kracher, J.Q. Yan, S.L. Bud'ko, P.C. Canfield, *Phys. Rev. B.* **82**, 014534 (2010)
26. N. Ni, A. Thaler, J.Q. Yan, A. Kracher, E. Colombier, S.L. Bud'ko, P.C. Canfield, S.T. Hannahs, *Phys. Rev. B.* **82**, 024519 (2010)
27. X. Zhuan, T. Qian, L. Li, J. Shen, L. Xiao, G. Cao, *Phys. C.* **470**(supplement 1), S447–S448 (2010). <http://www.sciencedirect.com/science/article/pii/S0921453409006121>
28. C.P. Bean, *Phys. Rev. Lett.* **8**, 250 (1962)
29. Y. Nakajima, Y. Tsuchiya, T. Taen, H. Yagyuda, T. Tamegai, S. Okayasu, M. Sasase, H. Kitamura, T. Murakami, *Physica C.* **470**, 1103 (2010)
30. M. Zehetmayer, M. Eisterer, H.W. Weber, J. Jiang, J.D. Weiss, A. Yamamoto, A.A. Polyanskii, E.E. Hellstrom, D.C. Larbalestier, *Phys. C.* **470**, S452 (2010)
31. R. Prozorov, M.A. Tanatar, N. Ni, A. Kreyssig, S. Nandi, S.L. Bud'ko, A.I. Goldman, P.C. Canfield, *Phys. Rev. B.* **80**, 174517 (2009)
32. A. Yamamoto, J. Jaroszynski, C. Tarantini, L. Balicas, J. Jiang, A. Gurevich, D.C. Larbalestier, R. Jin, A.S. Sefat, M.A. McGuire, B.C. Sales, D.K. Christen, D. Mandrus, *Appl. Phys. Lett.* **94**, 062511 (2009)
33. T. Taen, Y. Nakajima, T. Tamegai, H. Kitamura, *Phys. Rev. B.* **86**, 094527 (2012)
34. C.J. van der Beek, S. Demirdis, M. Konczykowski, Y. Fasano, N.R. Cejas Bolecek, H. Pastoriza, D. Colson, F. Rullier-Albenque, *Phys. B.* **407**, 1746 (2012)
35. F.L. Ning, K. Ahilan, T. Imai, A.S. Sefat, R. Jin, M.A. McGuire, B.C. Sales, D. Mandrus, *Phys. Rev. B.* **79**(R), 140506 (2009)
36. N. Fanlong, A. Kanagasingham, I. Takashi, A.S. Sefat, J. Ronying, M.A. McGuire, B.C. Sales, D. Mandrus, *J. Phys. Soc. Jpn.* **77**, 103705 (2008)
37. S. Oh, A.M. Mounce, S. Mukhopadhyay, W.P. Halperin, A.B. Vorontsov, S.L. Bud'ko, P.C. Canfield, Y. Furukawa, A.P. Reyes, P.L. Kuhns, *Phys. Rev. B.* **83**, 214501 (2011)
38. E. Granado, L. Mendonça-Ferreira, F. Garcia, G.M. de Azevedo, G. Fabbri, E.M. Bittar, C. Adriano, T.M. Garitezi, P.F.S. Rosa, L.F. Bufaiçal, M.A. Avila, H. Terashita, P.G. Pagliuso, *Phys. Rev. B.* **83**, 184508 (2011)
39. E.M. Bittar, C. Adriano, T.M. Garitezi, P.F.S. Rosa, L. Mendonça-Ferreira, F. Garcia, G.M. de Azevedo, P.G. Pagliuso, E. Granado, *Phys. Rev. Lett.* **107**, 267402 (2011)
40. P.F.S. Rosa, C. Adriano, T.M. Garitezi, R.A. Ribeiro, Z. Fisk, P.G. Pagliuso, *Phys. Rev. B.* **86**, 094408 (2012)
41. P.F.S. Rosa, C. Adriano, W. Iwamoto, T.M. Garitezi, T. Grant, Z. Fisk, P.G. Pagliuso, *Phys. Rev. B.* **86**, 165131 (2012)